

Maximizing Transmission Opportunities in Wireless Multihop Networks

Jeong-Yoon Lee, *Student Member, IEEE*, Chansu Yu, *Senior Member, IEEE*,
Kang G. Shin, *Fellow, IEEE*, and Young-Joo Suh, *Member, IEEE*

Abstract—Being readily available in most of 802.11 radios, multirate capability appears to be useful as WiFi networks are getting more prevalent and crowded. More specifically, it would be helpful in high-density scenarios because internode distance is short enough to employ high data rates. However, communication at high data rates mandates a large number of hops for a given node pair in a multihop network and thus, can easily be depreciated as per-hop overhead at several layers of network protocol is aggregated over the increased number of hops. This paper presents a novel multihop, multirate adaptation mechanism, called *multihop transmission opportunity* (MTO), that allows a frame to be forwarded a number of hops consecutively to minimize the MAC-layer overhead between hops. This seemingly collision-prone *nonstop forwarding* is proved to be safe via analysis and USRP/GNU Radio-based experiment in this paper. The idea of MTO is in clear contrast to the conventional opportunistic transmission mechanism, known as TXOP, where a node transmits multiple frames back-to-back when it gets an opportunity in a single-hop WLAN. We conducted an extensive simulation study via OPNET, demonstrating the performance advantage of MTO under a wide range of network scenarios.

Index Terms—Opportunistic communication, wireless multihop networks, medium access control, data rate adaptation, multirate routing

1 INTRODUCTION

MULTIHOP wireless networks pose more importance as we have seen various types of such networks on the horizon such as *wireless sensor networks*, *vehicular ad hoc networks*, and *wireless mesh networks* (WMNs), and more recently, network of *unmanned aerial vehicles* [2], [3] and *mobile social networks* (MSNs) [4], [5]. These emerging multihop networks exhibit characteristics that deviate significantly from the traditional ad hoc networks in terms of scale, traffic intensity, node density, and/or speed. For example, MSN scenarios typically envisaged around crowd spots, where the number of nodes within range could be hundreds or thousands [6]. A similar high-density scenario can also be observed in 802.11 deployments and WMNs in US cities.

Being readily available in most of 802.11 radios, multirate capability seems to be promising and can effectively exploits the short internode distance in high-density networks. However, it is important to observe that performance does

not improve linearly as data rate increases. This is due to the rate-independent overhead at the PHY and MAC layers, which are imposed by industry standards such as 802.11 [7]. Moreover, this overhead becomes more dominant as rate increases because the transmission time of the payload decreases proportionally (see Section 2.2).

Opportunistic transmission protocols (TXOP) [8], [9], [10], [11] have been proposed to alleviate the MAC-layer overhead by allowing a node to transmit multiple frames back-to-back when it transmits at high rate. A node is granted a dedicated time duration, which is called $TXOP_{limit}$ (3,264 or 6,016 μ s) in 802.11e [8], promoting *time-based fairness*. Figs. 1a and 1b show the benefit of TXOP in comparison to 802.11. In TXOP, node 0 is allowed to transmit multiple frames consecutively with just a short gap between frames (SIFS, 10 μ s), reducing the MAC overhead. However, TXOP is only applicable to WLANs and may defeat the usual expectation in multihop networks because 1) a node may not have multiple frames to transmit back-to-back although it is given an opportunity, 2) it can easily overload intermediate nodes in a multihop chain when a predecessor grabs more transmission opportunities than its successors, and 3) TXOP's time-based fairness is not appropriate in multihop networks as described in Section 2.4.

This paper proposes a novel frame forwarding mechanism, called *multihop transmission opportunity* (MTO), that extends the idea of TXOP in multirate, multihop networks. In MTO, a frame is forwarded over multiple hops (say, $0 \rightarrow 1$, $1 \rightarrow 2$, $2 \rightarrow 3$, etc.) with a single channel contention as shown in Fig. 1c. This reduces the MAC overhead and at the same time, resolves the above-mentioned problems of TXOP.

This paper extends our earlier work on MTO [1], particularly in the following three ways:

- J.-Y. Lee is with the Department of Computer Science and Engineering, Pohang University of Science and Technology, San 31, Hyoja-dong, Nam-gu, Pohang, Gyungbuk 790-784, Korea. E-mail: jylee9@postech.ac.kr.
- C. Yu is with the Department of Electrical and Computer Engineering, Cleveland State University, 2121 Euclid Avenue, Cleveland, OH 44115, and with the Division of ITCE, Pohang University of Science and Technology, Pohang, Korea. E-mail: c.yu91@csuohio.edu.
- K.G. Shin is with the Department of Electrical Engineering and Computer Science, University of Michigan, 2260 Hayward St. Ann Arbor, MI 48109-2121. E-mail: kgshin@umich.edu.
- Y.-J. Suh is with the Department of Computer Science and Engineering and with the Division of ITCE, Pohang University of Science and Technology, San 31, Hyoja-dong, Nam-gu, Pohang, Gyungbuk 790-784, Korea. E-mail: yjsuh@postech.ac.kr.

Manuscript received 26 June 2011; revised 10 Feb. 2012; accepted 29 June 2012; published online 10 July 2012.

For information on obtaining reprints of this article, please send e-mail to: tmc@computer.org, and reference IEEECS Log Number TMC-2011-06-0344. Digital Object Identifier no. 10.1109/TMC.2012.159.

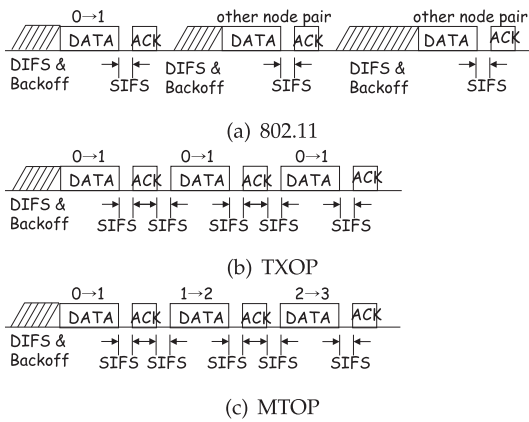


Fig. 1. Communication sequence in 802.11, TXOP and MTOP. (In (b), node 0 sends three back-to-back frames. In (c), nodes 0, 1, and 2 relay a frame back-to-back.)

- First, this paper presents a more accurate analysis on the maximum number of nonstop forwarding (h_i) (see Section 4.2).
- Second, several enhancements have been made to the original MTOP algorithm. For example, in Fig. 1c, node 1's nonstop forwarding to node 2 serves as an ack to node 0 (*implicit acknowledgment*), which is similarly approached in 802.11 PCF (point coordination function) [7] (see Section 4.4). Another enhancement is to (nonstop) forward frames in the order of their arrivals. This improves (*space-based*) fairness but also brings in complications too (see Section 4.3). One more major enhancement is to use *Srcr* [12] as an underlying multirate routing algorithm (see Section 4.5).
- Third, performance study has been expanded significantly. OPNET [13] is used instead of ns-2. *Ricean channel model* is additionally considered, traffic load is varied in two different ways, and also a variety of performance measures are used (see Section 5).

A small-scale experiment based on *universal software radio peripheral* (USRP) [14] and *GNU radio* [15] has been conducted with low-rate DBPSK (300 kbps) and high-rate DQPSK (600 kbps) modulation scheme. This shows that the additional transmission opportunity exists in multirate communication environment using the new concept called *multirate margin* and thus, that nonstop forwarding does not cause additional collisions due to this margin (see Section 5.1). Also, an extensive simulation study based on OPNET [13] has been presented (see Sections 5.2 and 5.3). Our evaluation study has indicated that MTOP outperforms fixed-rate cases (DSR1 and DSR11) as well as *Srcr* in most of the simulation scenarios tested. Compared to *Srcr*, MTOP improves the packet delivery ratio (PDR) by as much as 13.8 percent and the average end-to-end packet delay is reduced by 12-43 percent. The performance gain is contributed most by a significant reduction in packet drops (43.7-150.5 percent less drops than *Srcr*) and MAC overhead.

The remainder of the paper is organized as follows: Section 2 overviews the characteristics of multirate radio and discusses performance anomaly in multirate networks.

Section 3 analyzes the defer threshold at different data rates, and quantitatively provides the multirate margin via analysis. Section 4 describes the proposed protocol, MTOP, which is followed by GNU Radio/USRP-based experiment and OPNET-based evaluation in Section 5. The paper concludes with Section 6.

2 BACKGROUND AND RELATED WORK

2.1 Multirate Support in IEEE 802.11 Standards and Rate Adaptation Algorithms

According to IEEE 802.11 PHY-layer specifications [7], it supports 2.4-GHz *direct sequence spread spectrum* at the data rate of 1 and 2 Mbps while a later standard, IEEE 802.11b, supports the additional data rate of 5.5 and 11 Mbps that tradeoff interference tolerance for performance. 802.11a/g supports 6, 9, 12, 18, 24, 36, 48, and 54 Mbps.

There have been a number of proposals on multirate algorithms for 802.11-based WLANs in the literature. *Autorate fallback* (ARF) [16] is the first multirate algorithm, the basic idea of which is to use a higher rate upon consecutive successful transmissions and to fall back to a lower rate after a number of consecutive transmission failures. Variations of the ARF includes *adaptive ARF* [17], *adaptive multirate retry* [17], and *estimated rate fallback* [18]. In *receiver-based autorate* [19], the receiver estimates the channel quality based on the SINR of the received RTS frame, determines the best data rate that the transmitter must use and then, informs it by piggybacking in the CTS packet. *Opportunistic autorate* protocol [9] exploits durations of high-quality channel conditions and sending multiple back-to-back data packets without gaps. This is similarly approached in *medium access diversity* [20].

Since this paper concentrates on multihop networks, it is important to discuss rate-aware multihop routing algorithms in the literature. Typically, they have concentrated on developing a rate-aware link cost which is then integrated with a multihop routing algorithm to find the path that minimizes the total cost. Link costs used include delay [21], *bandwidth distance product* [22], *medium time metric* [23], *estimated transmission time* (ETT) [12], *weighted cumulative ETT* [24], and *bandwidth delay product* [25]. Most of previous studies employ *proactive* routing algorithms such as *destination-sequenced distance vector* [26]. On the other hand, *Srcr* [12] and *MR-LQSR* [24] rely on on-demand routing principles borrowed from *dynamic source routing* (DSR) [27].

2.2 PHY- and MAC-Layer Overheads

To understand the PHY- and MAC-layer overhead, let t_i be the transmission time of a PHY frame for a 512-byte payload at rate i and T_i be the time duration of the frame sequence at MAC. Note that a PHY frame is composed of PLCP preamble/header and the payload, where the former shall be transmitted using the lowest data rate (1 Mbps) while the latter is transmitted at a higher rate. Since the PLCP preamble/header are 192 bits (192 μ s), the overall frame size is 4,288 μ s at 1 Mbps (t_1). Since the payload can be transmitted at higher rates, it becomes 2,240 μ s (t_2), 937 μ s ($t_{5.5}$), and 564 μ s (t_{11}) for 2, 5.5, and 11 Mbps, respectively.

To estimate T_i , we assume no RTS/CTS exchange and assume a high traffic condition in which every frame

transmission contend for medium access by waiting for a random time chosen within the *contention window* (CW). CW is 31-1,023 and slot time is 20 μ s. The time for contention on the average is $\frac{31 \times 20}{3}$ or 207 μ s when CW is 31 with two contending nodes. Here is the explanation on the denominator, 3. With two contending nodes, they choose random slots within the contention window (620 μ s). Since the losing station (that chooses the larger slot) uses the remaining backoff time, the sum of the contention time of the two stations is same as that of the losing station, which is two thirds of the contention window. Therefore, the average contention time for both the winning and losing station is calculated as $\frac{1}{3}$ of the contention window.

Now, the time duration for the frame sequence at data rate i , T_i , consists of DIFS and contention (t_c or 50 + 207 μ s), Data (t_i), SIFS (t_{SIFS} or 10 μ s) and ACK (t_{ACK} or 304 μ s), i.e.,

$$T_i = t_c + t_i + t_{SIFS} + t_{ACK}. \quad (1)$$

It totals 4,859 μ s (T_1), 2,811 μ s (T_2), 1,508 μ s ($T_{5.5}$), and 1,135 μ s (T_{11}) for 1, 2, 5.5, and 11 Mbps, respectively.

Now, per-frame PHY overhead due to PLCP preamble/header is 4.5, 8.6, 20.5, and 34.0 percent at 1, 2, 5.5, and 11 Mbps. The MAC-layer overhead amounts to 11.8, 20.3, 37.9, and 50.3 percent for 1, 2, 5.5, and 11 Mbps, respectively. Efforts have been made to reduce the PHY and MAC overheads. For example, a later standard 802.11b introduces a shorter PLCP preamble (72 bits) and allows the PLCP header (48 bits) to transmit at 2 Mbps for high-rate transmission (5.5 and 11 Mbps). Also, 802.11a/g reduce the MAC overhead by adopting a smaller CW (15-1,023) as well as a smaller slot size (9 μ s).

On the other hand, the MAC overhead can be reduced by directly reducing the overhead including the backoff time or indirectly reducing it based on collision avoidance or collision masking. One of the latter is packet salvaging at the MAC. Biswas and Morris [28] proposed *extremely opportunistic routing*, in which a collided packet can be saved by intermediate nodes that can be effective in wireless environment with abundant temporary link errors. This is similarly approached in [29]. Direct approaches include *Sift* [30], which uses a carefully chosen, nonuniform probability distribution of transmitting in each slot within the contention. The most relevant to our approach is *aggregation with fragment retransmission* [31] as it addresses the problem of relatively large overhead at high data rates. That is, it mitigates the overhead by supporting transmissions of very large frames and partial retransmissions in the case of errors.


2.3 Transmission Opportunity and Performance Anomaly

Another important development in reducing the MAC overhead is *transmission opportunity* (TXOP), which allows a node to transmit multiple frames with a single channel access. This was originally proposed in 802.11e to improve *fairness* by granting a node with a lower channel access priority a dedicated time duration, which is called $TXOP_{limit}$ (3,264 or 6,016 μ s) [8].

In fact, the fairness problem and the associated *performance anomaly* have been observed by many researchers in


TABLE 1
Performance Anomaly

(a) Single-hop scenario



	A-B	C-D
Throughput (Mbps, 802.11)	0.683	0.683
Medium time (% , 802.11)	81	19
Throughput (Mbps, TXOP)	0.527	1.581
Medium time (% , TXOP)	63	37

(b) Multihop scenario



	A-B	C-D
Throughput (Mbps, 802.11)	0.595	0.198
Medium time (% , 802.11)	69	31
Throughput (Mbps, TXOP)	0.393	0.393
Medium time (% , TXOP)	46	54
Throughput (Mbps, MTO)	0.527	0.527
Medium time (% , MTO)	63	37

In (a), A-B: 1 Mbps, 272 m, C-D: 11 Mbps, 118 m; in (b), A-B: 1 Mbps, 272 m, C-to-D: 11 Mbps, 118 m each hop.

the context of multirate WLANs [10], [11], [32]. While 802.11 MAC guarantees that each node gets an equal chance of transmitting its frames, it does not necessarily mean that each node gets an equal share of the channel (time) in a multirate environment. With TXOP, a low-rate node pair is not impacted significantly in terms of throughput but a high-rate node pair is benefited significantly.

To demonstrate this *time-based fairness*, consider an example scenario in Table 1a for a mixture of low ($A \leftarrow B$) and high-rate ($C \rightarrow D$) communication. B transmits one 512-byte frame during T_1 or 4,859 μ s and C does one during T_{11} or 1,135 μ s. Assuming that the two transmitters get equal chance of medium access, the aggregate throughput is

$$\frac{\text{Two } 512B \text{ frames}}{T_1 + T_{11}} = 1.37 \text{ Mbps}, \quad (2)$$

which is barely larger than the lower data rate. Moreover, C - D node pair is not fairly treated because it uses only 19 percent of medium time ($\frac{T_{11}}{T_1 + T_{11}}$).

TXOP improves the situation. Let us first compute the maximum allowable number of frames (k_i) to transmit consecutively at data rate i during $TXOP_{limit}$. Since SIFS (t_{SIFS}) replaces DIFS and contention (t_c) between k_i consecutive frames, k_i can be obtained as follows:

$$\begin{aligned} \max_{k_i} (k_i \cdot T_i - (k_i - 1) \cdot t_c \\ + (k_i - 1) \cdot t_{SIFS} \leq TXOP_{limit}). \end{aligned} \quad (3)$$

When $TXOP_{limit}$ is 3,264 μ s [8], k_i is 1 for 1 and 2 Mbps, 2 for 5.5 Mbps, and 3 for 11 Mbps. Now, while node B transmits one frame (k_1) during T_1 , node C transmits three frames (k_{11}) consecutively during $T'_{11} = 3 \cdot T_{11} - 2 \cdot t_c + 2 \cdot t_{SIFS}$ or 2,911 μ s. Therefore, the aggregate throughput is improved to

$$\frac{\text{Four } 512B \text{ frames}}{T_1 + T'_{11}} = 2.11 \text{ Mbps}. \quad (4)$$

TABLE 2
Characteristics of an 802.11b Multirate Radio

Data rate (Mbps)	1	2	5.5	11
Receive sensitivity (dBm)	-94	-91	-87	-82
Range or r_i (m)	272	221	167	118
SIR requirement (dB)	2.2	5.2	4.4	7.6
Max. interference (dBm)	-96.2	-96.2	-91.4	-89.6
Min. RI distance (m)	317	317	227	200
Min. TI distance (m)	589	538	394	318
Required defer threshold (dBm)	-105.1	-103.8	-99.3	-96.2
Defer threshold (dBm)	-105.1			

Transmit power: 15 dBm, indoor radio propagation model with path loss exponent of 3.3 [35]. Values in the last six rows are for target BER of 10^{-5} .

More importantly, C - D node pair uses 37 percent of medium time, which is a significant improvement in terms of fairness. Please refer to Table 1a for summary.

2.4 Multihop Anomaly

In a multihop network, the problem becomes more complicated due partly to interhop interference and rate-hop count tradeoff. Consider an example in Table 1b, where B wants to talk to A at 1 Mbps and C wants to talk to D at 11 Mbps with two intermediate nodes, E and F . Note that the communication range at 1 and 11 Mbps is 272 and 118 m, respectively, and the carrier sense range is 589 m as detailed later in this paper (see Table 2).

Two transmitters (B and C) and two intermediate nodes (E and F) can sense each other and thus, they will get an equal chance for medium access as long as they have packets to transmit. When only B and C are ready, they transmit one packet each. When B , C , and E are ready, they transmit one each, which is similarly the case when B , C , E , and F are ready. Assuming that those cases occur with the same probability and that two source nodes, B and C , always have packets to transmit, one destination A receives three packets while another destination D receives one.

With 802.11, the aggregate end-to-end throughput will be

$$\frac{\text{Four } 512B \text{ frames}}{3 \cdot T_1 + 6 \cdot T_{11}} = 0.79 \text{ Mbps}, \quad (5)$$

and C - D node pair occupies $\frac{6 \cdot T_{11}}{3 \cdot T_1 + 6 \cdot T_{11}}$ or 31 percent of medium time, which indicates a serious fairness problem. Here, t_c becomes $174 \mu\text{s}$ because there exist four contending nodes instead of two. Correspondingly, T_1 and T_{11} are $4,776$ and $1,052 \mu\text{s}$, respectively.

Interestingly, TXOP improves fairness in multihop networks too but does not increase the throughput unlike in single-hop networks. Since C , E , and F will transmit three frames at once during T'_{11} each, the aggregate end-to-end throughput will be

$$\frac{\text{Six } 512B \text{ frames}}{3 \cdot T_1 + 6 \cdot T'_{11}} = 0.79 \text{ Mbps}, \quad (6)$$

and C - D node pair occupies $\frac{6 \cdot T'_{11}}{3 \cdot T_1 + 6 \cdot T'_{11}}$ or 54 percent of medium time. In other words, TXOP trades throughput in favor of fairness. More seriously, A - B pair achieves only two thirds of the throughput in comparison to 802.11 in

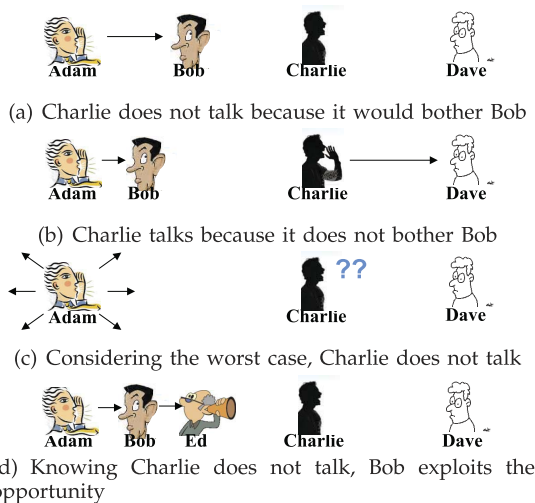


Fig. 2. The defer-if-hear-anything principle. (Multihop forwarding is drawn in (d).)

Table 1b. Unlike in single-hop networks, TXOP greatly impacts the low-rate communication.

Therefore, it is necessary to apply the idea of opportunistic transmission in a different manner in multihop environment. The multihop opportunistic transmission algorithm proposed in this paper allows nodes E and F to forward a frame with no additional contention. In other words, C , E , and F will transmit/forward a frame back-to-back during T'_{11} . Therefore, the aggregate end-to-end throughput becomes

$$\frac{\text{Two } 512B \text{ frames}}{T_1 + T'_{11}} = 1.05 \text{ Mbps}, \quad (7)$$

which is 34 percent higher than TXOP and at the same time equally shared by two flows (A -to- B and C -to- D), improving the fairness compared to 802.11.

3 MULTIRATE MARGIN

MTOP encourages nonstop forwarding of a frame over multiple hops as discussed in Section 1. It seems apparent that collisions are abundant because intermediate relay nodes do not appropriately compete for a chance to use the shared medium. However, when the first node in the multihop chain is given an exclusive right based on the underlying MAC protocol, it in fact inhibits a larger set of nodes than necessary, which is enough to keep the next hop communications from interference if it is transmitted at "high rates." The corresponding quantitative measure is called *multirate margin* in this paper.

3.1 An Illustrative Example

Before describing the multirate margin in detail, this section presents an illustrative example that explains the multirate margin and multihop forwarding mechanism in the proposed MTOP protocol. Consider the voice communication scenario among four persons as in Fig. 2 Adam, Bob, Charlie, and Dave. Adam wants to talk to Bob and Charlie wants to talk to Dave. They use the same *defer-if-hear-anything* principle (like CSMA) and nonnegligible intermessage pause (like DIFS and backoff) to avoid collisions.

In Fig. 2a, when Adam talks to Bob, Charlie would not begin his conversation to Dave because he knows it would interfere with Adam-Bob's communication (analogous to low defer threshold at 1 Mbps). In Fig. 2b, Charlie would begin his conversation because he knows it would not interfere with Adam-Bob's communication (high defer threshold at 11 Mbps). In reality, however, Charlie does not know whom Adam talks to but just overhears Adam's voice as shown in Fig. 2c. Considering the worst case scenario, Charlie would not begin his conversation until Adam completes (a lower one is specified as the defer threshold). Now, here is the interesting part. In Fig. 2d, knowing that Charlie would not talk, Bob exploits this opportunity to immediately forward the message to Ed. Time is saved because Bob does not "pause" between the messages.

3.2 Receive Sensitivity and SINR Requirement

Steps to analyze the multirate margin are as follow:

1. Estimate the communication range (r_i) based on the receive sensitivity at different rates.
2. Estimate the SIR requirement using analysis.
3. Receive sensitivity is subtracted from the SIR requirement for target BER of 10^{-5} to estimate the maximum tolerable interference, which translates to the minimum RI (receiver to interference) distance.
4. This is added to the communication range to estimate the minimum TI (transmitter to interferer) distance, which is translated to the required defer threshold at different rates based on the transmit power and path loss model.
5. Finally, multirate margin is the difference between the *defer threshold* at 1 Mbps and the required defer threshold at high rates. Table 2 summarizes the results. Note that this is not our own development for the sake of MTOP but is the case in practice [16].

Step 1: For a successful communication, the received signal power must be higher than the *receive sensitivity* in the presence of path loss over distance. Table 2 shows them at four data rates of 2.4 GHz 802.11b radio [33]. Indoor path loss model by Marquesse [34] has been used to derive the "communication range," i.e., path loss = $40.2 + 20 \cdot \log_{10}(d)$ if $d \leq 8$ m, and $58.5 + 33 \cdot \log_{10}(d/8)$, otherwise.

Step 2: Moreover, the received signal power must be strong enough to overcome the influence of noise and interference from all other simultaneous transmissions, i.e., SINR must be higher than a certain threshold [36]. A higher rate communication requires a higher threshold, which means that it is more subjective to interference. Based on the study in [35], BER calculation for 802.11b 1 Mbps is as follows:

$$BER_1 = Q(\sqrt{11 \cdot SIR}), \quad (8)$$

where Q function is defined as

$$Q(x) = \frac{1}{\sqrt{2\pi}} \int_x^{\infty} e^{-\frac{t^2}{2}} dt. \quad (9)$$

BER calculation for 802.11b 2, 5.5, and 11Mbps are given as follows:

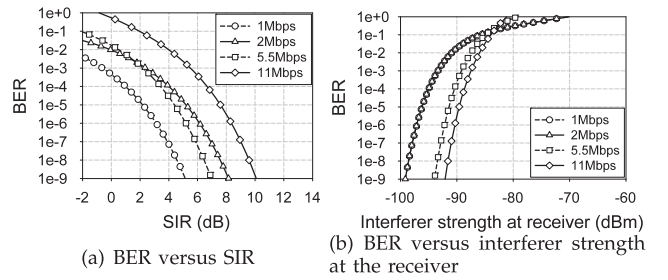


Fig. 3. Multirate margin. (b shows the highest tolerable interference when the signal strength at the receiver is equal to the receive sensitivity.)

$$BER_2 = Q(\sqrt{5.5 \cdot SIR}), \quad (10)$$

$$BER_{5.5} \leq \frac{2^4 - 1}{2^4 - 1} (14 \cdot Q(\sqrt{8 \cdot SIR}) + Q(\sqrt{16 \cdot SIR})), \quad (11)$$

and

$$BER_{11} \leq \frac{2^8 - 1}{2^8 - 1} (24 \cdot Q(\sqrt{4 \cdot SIR}) + 16 \cdot Q(\sqrt{6 \cdot SIR}) + 174 \cdot Q(\sqrt{8 \cdot SIR}) + 16 \cdot Q(\sqrt{10 \cdot SIR}) + 24 \cdot Q(\sqrt{12 \cdot SIR}) + Q(\sqrt{16 \cdot SIR})). \quad (12)$$

Fig. 3a shows the BER curve for four different data rates. The "SIR requirement" for target BER of 10^{-5} is shown in Table 2. Note that we use SIR instead of SINR as in [35] because interference is generally much stronger than noise [37] and the capacity of multihop networks is determined by the communication robustness in the presence of cochannel interference.

3.3 Defer Threshold and Multirate Margin

Step 3: Assume that the signal strength at the receiver is equal to the receive sensitivity in Table 2, Fig. 3b shows the maximum tolerable interference to meet the SIR requirement of Fig. 3a. Those for the target BER of 10^{-5} are shown in Table 2 along with the equivalent "RI distance." For instance, nodes within 317 m from a 1 Mbps "receiver" must not transmit concurrently as drawn in Fig. 4a; otherwise, the T-R communication will fail due to the lower SIR than required.

Step 4: To refrain a potential interferer from transmitting, *defer threshold* is employed. In other words, an 802.11 PHY performs *clear channel assessment*, which involves declaring the channel busy if it detects any signal energy above the pre-specified defer threshold [38].

However, since the receiver does not transmit signals, the minimum TI distance from the previous step (or the corresponding signal threshold) cannot be implemented. Instead, this can only be mandated in practice by sensing the signal from the transmitter. Therefore, nodes within 589 m from a 1 Mbps "transmitter" are forbidden from transmitting concurrently as in Fig. 4a, which is obtained by adding the communication range (r_1) to the RI distance [39]. This "minimum TI distance" is translated to the defer threshold by using the indoor path loss model and the transmit power of 15 dBm.

Step 5: Repeating the steps 1-4 above at different rates provides different communication range, SIR requirement, min RI distance, and min TI distance (and correspondingly,

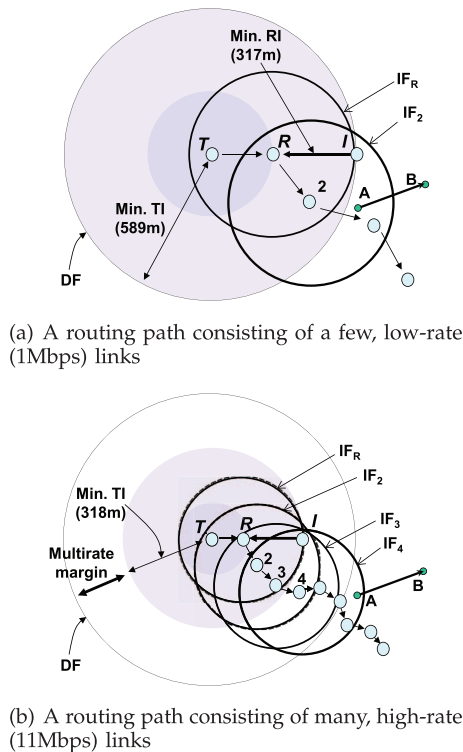


Fig. 4. Multirate margin and the MTOP mechanism. (Nonstop forwarding $R \rightarrow 2$ will not be successful in (a) because $A \in IF_2$ but will be okay in (b) because $A \notin IF_2$.)

the required defer threshold) as summarized in Table 2. Fig. 4b shows the case for 11 Mbps. Now, notice that potential interferers are oblivious of the data rate that the transmitter use and thus, it is unavoidable to employ the same, lowest threshold [22] (like Charlie in Fig. 2c). This is -105.1 dBm as in Table 2 and the corresponding range is denoted as DF in Fig. 4.

Since the required defer threshold at 11 Mbps is -96.2 dBm, there exists an 8.9 dB margin, which we call *multirate margin* in this paper. In other words, “*multirate margin*” is defined as the difference between the pre-specified defer threshold (for the lowest rate transmission) and the required defer threshold for high-rate transmission.

4 MULTIHOP TRANSMISSION OPPORTUNITY (MTOP)

4.1 Multihop Nonstop Forwarding

The MTOP protocol exploits the above-mentioned multirate margin by allowing a frame to travel a few more hops with a single medium access. In Fig. 4b, while node T transmits a frame to node R , node A is allowed to transmit its own frame to node B because A is outside of DF , i.e., $A \notin DF$. When node R forwards the frame to node 2 based on the MTOP mechanism, it would not be interfered with because $A \notin IF_2$. (Here, IF_i denotes the interference range of node i , which is determined based on the min RI distance.) This holds true for the next node ($A \notin IF_3$) but not for the following hop node ($A \in IF_4$).

In other words, when node T transmits data frame at 11 Mbps, most of potential interferers for the current communication ($T \rightarrow R$) as well as the next two hop

communications ($R \rightarrow 2$ and $2 \rightarrow 3$) would be inhibited. This is due to the additional 8.9 dB margin discussed in the previous section. On the other hand, this is not the case for communication at low-rate. As shown in Fig. 4a, node R 's (nonstop) forwarding to node 2 will be interfered with A 's transmission because $A \in IF_2$.

We define $MTOP_{limit}$ as the remaining margin that a node can exploit for successive transmission to the next hop without an additional contention for medium access. While $TXOP_{limit}$ is measured in time and is associated with a node as discussed in Section 2.3, $MTOP_{limit}$ is measured in dB and is associated with a frame. However, similar to $TXOP_{limit}$, $MTOP_{limit}$ can be translated to the number of hops or distance, for convenience. That is, each node decides that it can make additional MTOP forwarding if the remaining margin is sufficient for the next hop transmission at the given data rate i , i.e.,

$$MTOP_{limit} - r_i > Min. RI \text{ distance}_i. \quad (13)$$

This is based on the conservative assumption that each transmission makes the farthest possible progress (r_i) at the specified data rate. The remaining multirate margin is initialized to $Min. TI \text{ distance}_{e_1}$ at the first node of the forwarding chain and is updated as $MTOP_{limit} = MTOP_{limit} - r_i$.

To avoid collision from hidden terminals, MTOP optionally uses RTS/CTS as in 802.11. However, it is used only for the first transmission in MTOP but not for the following nonstop forwarding. In other words, node T and R exchanges RTS and CTS before transmitting a data packet in Fig. 4b but node R nonstop-forwards the packet without the virtual carrier sensing. Note that RTS/CTS helps reduce the collisions but it has not been widely used in practice due to the corresponding overhead. This overhead is not as significant in MTOP because more than a half of all communications are nonstop-forwarded in MTOP as observed in Section 5.3.

4.2 Number of Multihop Forwarding (h_i)

When every hop communication is at rate i , the number of hops (h_i) to nonstop-forward is

$$h_i = \left\lfloor \frac{Min. TI \text{ distance}_{e_1} - Min. RI \text{ distance}_i}{r_i} \right\rfloor. \quad (14)$$

According to parameters in Table 2, h_i is one for 1 and 2 Mbps, two for 5.5 Mbps, and three for 11 Mbps.

However, the h_i calculation is considered pessimistic and could be larger because intermediate nodes ($T, R, 2$, and 3 in Fig. 4b) neither lie at a straight line nor at the edge of the communication range. To better estimate h_i , consider Fig. 5, where node 0 transmits to node 1. Node 0 desires to make the farthest progress toward the destination within its transmission range r . However, it is unable to achieve that far due to the sparsity of nodes in the neighborhood. Here, we analyze the expected value of the progress as a function of node density.

Let node 1 be the next hop node, which makes the progress of x toward the destination as shown in the figure. Expected value of x or $E[X]$ can be computed as

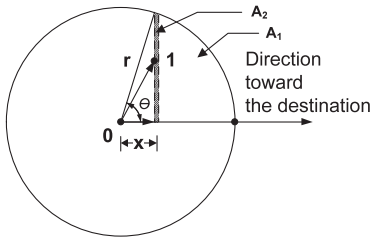


Fig. 5. h_i analysis. (h_i depends on x , which in turn depends on node density, λ , and transmission range, r .)

$E[x] = \int_0^r x f_X(x) dx$, where $f_X(x)$ denotes the probability density function of x . Since node 1 is chosen because no other node is found in A_1 ,

$$\begin{aligned} f_X(x) \Delta x &= p(x \leq X \leq x + \Delta x) \\ &= Pr\{\text{no node in } A_1\} \cdot Pr\{\text{at least one node in } A_2\} \\ &= e^{-\lambda A_1} (1 - e^{-\lambda A_2}), \end{aligned} \tag{15}$$

assuming that node locations follow Poisson distribution with node density (λ). Here, $A_1 = \theta \cdot r^2 - r \cdot \sin \theta \cdot x$ and $A_2 = 2r \cdot \sin \theta \cdot \Delta x$ taking into account both the upper and the lower half of the circle in the figure.

$E[X]$ is used in place of r_i in (13) and (14). Our calculation shows that h_i becomes 3 for 5.5 Mbps and 8 for 11Mbps when node density is 30 nodes in $300 \times 1,500 \text{ m}^2$ ($\lambda = 6.67 \times 10^{-5}$) and 2 and 4 when the number of nodes is 110 ($\lambda = 2.44 \times 10^{-3}$). In practice, λ can be estimated, for example, based on the number of neighboring nodes.

4.3 Space-Based Fairness

Another important issue with MTOP is fairness. As discussed in Sections 2.3 and 2.4, time-based fairness in 802.11 and TXOP is not appropriate in multihop environment. For example, a node that transmits at high-rate contributes to the network by reducing the channel occupancy time but is disadvantaged by making less progress toward its respective destination due to the rate-distance tradeoff, creating a possibility of unfairness.

This paper introduces *space-based fairness*, which we claim is more appropriate in multirate, multihop networks. Here, the fairness is measured by the quantity of “work” that moves an object (packet) over the distance toward the destination. Applying it to end-to-end flows, it is considered perfectly fair when, for example, a pair of nodes separated by 100 m end-to-end achieves 100 packets while another pair separated by 400 m achieves 25 packets. In other words, $\gamma_i \cdot dist_i$ is the “total work” done on behalf of flow i and is desired to be balanced among the flows, where γ_i and $dist_i$ are the number of received packets and the end-to-end distance for flow i , respectively. The MTOP mechanism proposed in this paper facilitates the space-based fairness because a packet transmitted at high rate is given additional opportunity to travel further and thus, to achieve the same work.

One concern regarding fairness is that a node could (nonstop) forward a packet earlier than others in the packet queue. In MTOP, the node does not forward the newly arriving packet when it is given an opportunity.

Instead, it puts the packet in the packet queue and attempts to transmit the head of the queue. Some opportunities can be lost when the head of the queue is not a high-rate packet but fairness at a node is improved. It is also important to note that control frames such as probe packets always get a higher priority than (normal and nonstop-forwarded) data packets.

4.4 Implicit ACK

As an optimization technique, MTOP allows intermediate nodes to skip an explicit ACK and to use the immediate (nonstop) forwarding of a frame as an implicit ACK. Since the immediate forwarding occurs an SIFS after the previous transmission, it coincides with an explicit ACK in terms of frame schedule. However, it is clear that the last node in the chain of MTOP forwarding must transmit an explicit ACK. (It is interesting to compare this to Block Ack mechanism in TXOP [8].)

Two important questions in the implementation of the implicit ACK are as follows: 1) What if a predecessor does not receive an implicit ACK although the next node forwards the frame? 2) What if the next node forwards the data frame at a higher rate than the predecessor can receive?

The latter problem can easily be resolved by using an explicit ACK in such a case. As for the former, the predecessor retransmits the same frame, which is a duplicate to the next node. Such duplicate frames can be filtered out within the intermediate’s MAC based on the original functionality of the 802.11 MAC, called *duplicate frame filtering* [7]. This algorithm matches the sender address and the sender-generated sequence control number of a new frame against those of previously received ones. If there is a match, the receiver transmits ACK but ignores the duplicate frame. According to our simulation study detailed in the next section, the duplicate frames are less with MTOP.

4.5 Multirate Routing

MTOP uses Srcr, which is the default multirate routing protocol for MIT Roofnet [12]. It is based on DSR with link cache and tries to find the shortest route using Dijkstra’s algorithm on its link cache. The quality of a route is calculated as sum of ETT of each link. More specifically, each node broadcasts *probe* packets at every data rate every one second (with jitter) [12]. Then, its neighbors count the number of probe packets received within the probe window (e.g., 10 seconds) to estimate the quality of the corresponding wireless links in terms of ETT. As in DSR, intermediate nodes forward an RREQ to discover a route to the destination. In Srcr, they forward an RREQ if the route quality (i.e., sum of link ETTs) is lower than the previously identified value.

In our implementation of Srcr and MTOP, the size of probe packet is set to the same as normal data packet (e.g., 512B) as in [12] to estimate the ETT for a data packet correctly. Since the ETT metric favors higher data rates than the traditional hop count metric, both Srcr and MTOP would result in routing paths consisting of more number of high-rate links.

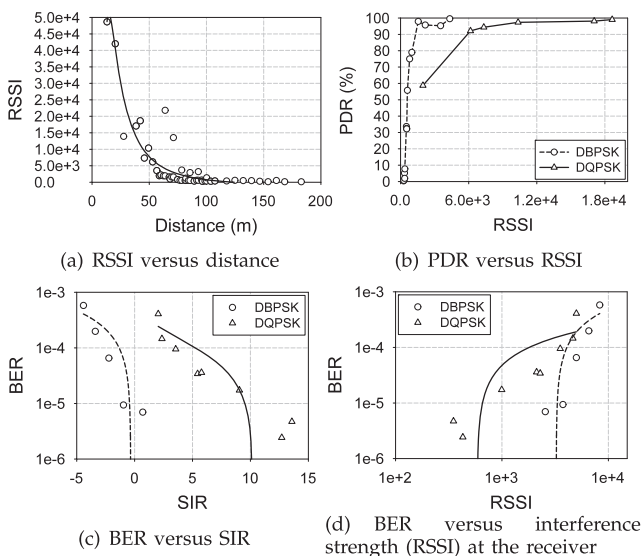


Fig. 6. USRP/GNU radio-based experimental results.

5 PERFORMANCE EVALUATION

5.1 Multirate Margin via USRP/GNU Radio-Based Experimentation

Since radio propagation and its channel dynamics cannot easily be captured using analytical or simulation models, we conducted an experimental study to demonstrate the multirate margin based on a small-scale testbed using USRP [14] and GNU Radio [15].

The following are the details of the experiment (see [40] for a similar setup):

1. The testbed includes three USRP systems (version 5b), three RFX2400 transceivers (2.3-2.9 GHz) and GNU Radio software (version 3.1.3).
2. Modulation schemes used are DBPSK (low-rate) and DQPSK (high-rate).
3. Carrier frequency and bandwidth we have tested are 2.4835 GHz and 300 KHz, respectively. Therefore, the maximum data rate is 300 and 600 Kbps for DBPSK and DQPSK, respectively. A smaller bandwidth and data rates are used partly due to bandwidth constraints imposed by the USRP [41].
4. Transmitter amplitude is set to 8,000, which is smaller than the default value (12,000). This is to make the communication range no farther than 300 feet.¹
5. Packet size is 1,500 bytes and 3,300 packets were transmitted for each experiment.

Our goal is to observe a similar trend as in Table 2, particularly the multirate margin with two data rates supported by DBPSK and DQPSK modulation schemes. The experiment has been conducted in two phases. First, to obtain communication range (r_i) with DBPSK and DQPSK, we set up two USRP systems and measured *received signal strength indicator* (RSSI) versus distance and PDR versus RSSI.² According to our experimental results in Figs. 6a

1. This experiment was conducted in the Edgewater Park near Lake Erie in Cleveland, Ohio.

2. Note also that RSSI obtainable from USRP/GNU Radio is “digital RSSI” value, meaning that it is based on the output of the analog-to-digital converter, which is not the true RF power at the antenna [42].

and 6b, r_i for DBPSK and DQPSK is estimated as 215 and 150 ft, respectively. Note that 90 percent PDR is used to estimate the communication range, which is equivalent to BER of 10^{-5} .

Second, to obtain the minimum RI distance, we set up three USRPs, a transmitter (T), a receiver (R), and an interferer (I) on a straight line (T - R - I). The TR distance is fixed to the communication range, i.e., 215 and 150 ft for DBPSK and DQPSK, respectively. Figs. 6c and 6d show BER versus SIR and BER versus RSSI (from I to R), which must be compared to Figs. 3a and 3b, respectively. Note that SIR at the receiver is calculated as RSSI from the sender minus RSSI from the interferer [43]. Note also that the observed SIR gap in Fig. 6c is larger than the theoretical gap of 3 dB. We believe this is due to the small number of measurements.

According to the experiment results, we observed that the low-rate communication (DBPSK) is more robust to interference than high-rate (DQPSK) as similarly observed in [41]. Minimum RI distance is estimated as 220 and 235 ft for DBPSK and DQPSK, respectively, and the minimum TI distance for 90 percent PDR is about 435 and 385 ft. Comparing to Table 2, we can conclude that the same trend and the multirate margin at a high rate (435 versus 385 ft) has been observed.

5.2 Simulation Environment

It is generally understood that the implementation of CSMA is hard for the current USRP/GNU radio platform due to hardware limitations [44], [45], [46]. For this and other practical reasons, the detailed analysis of MTOP performance is conducted via OPNET [13], which simulates node mobility, a realistic physical layer, radio network interfaces, and the 802.11 MAC protocol.

We compare four different schemes: fixed data rate of 1 and 11 Mbps with DSR (denoted as DSR1 and DSR11, respectively), Srcr, and MTOP. In fixed rate cases, every data packet is transmitted at the specified data rate. In a sparse network (e.g., 30 nodes in the network), we expect DSR11 suffers most because of the connectivity problem. But it will become advantageous as N increases. Performance metrics are 1) PDR and 2) average packet delay. Since MTOP potentially causes additional collisions, we also report 3) total number of transmissions, 4) total frame drops, 5) duplicate frames and 6) mixture of data rates used, all measured at the MAC layer.

Our evaluation is based on the simulation of 30-110 mobile nodes located in an area of $1,500 \times 300 \text{ m}^2$. The data traffic simulated is *constant bit rate* (CBR) traffic. At default, 30 CBR sessions are simulated at the rate of five 512B packets/second. However, a larger number of CBR sessions and a higher packet rate are also simulated to see the impact of traffic intensity on performance. To better understand the adaptive behavior of MTOP under different channel condition, Ricean channel model is also simulated. No mobility is assumed to clearly see the performance improvement due to the nonstop forwarding of MTOP. (Results with mobility are reported in our earlier work [1].) Simulation time is 900 seconds for each run and 10 simulation runs are repeated for each simulation scenario to obtain more accurate results.

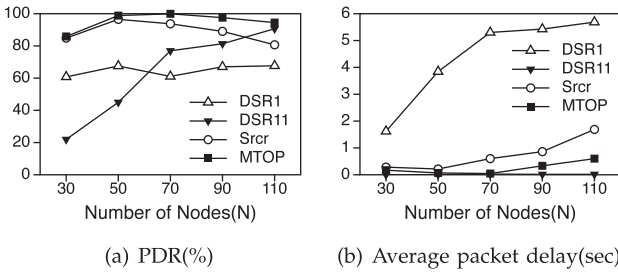


Fig. 7. Performance of MTOp in comparison to fixed rate cases (DSR1 and DSR11) and Srcr.

The aforementioned simulation parameters are typical in many previous studies on mobile ad hoc networks including [47] except that the traffic intensity and the number of nodes (N) are higher than usual. The traffic intensity of 30 sessions with 5 packets/second each could be overwhelming at 1 Mbps but it can be reasonably handled at 5 or 11 Mbps. N is as many as 110 in our simulation study because it allows more chances to use high data rates.

Note that the size of a probe message is set to the same as normal data packet (e.g., 512B) as described earlier. Since each node transmits one every second at every rate, the corresponding control overhead could be significant when N is large. Note that DSR1 and DSR11 do not have such overheads.

5.3 Simulation Results

5.3.1 PDR and Delay

Fig. 7 compares PDR and average packet delay of DSR1, DSR11, Srcr, and MTOp. Fig. 7a shows the PDR versus N . DSR11 does not function well as shown in the figure, particularly with a small N . This is due mainly to the lack of end-to-end connectivity. However, its performance increases rapidly as N increases. In DSR1, PDR stays almost constant regardless of N .

Srcr in general achieves a better performance than DSR1 and DSR11 because it uses a combination of all available data rates to maximize the network performance. However, as shown in Fig. 7a, when N is larger than 90, DSR11 performs better than Srcr. It is not surprising because of the extra overhead due to probe messages in Srcr (and MTOp). On the other hand, MTOp outperforms DSR1, DSR11, and Srcr in the entire range of N simulated as shown in Fig. 7a. MTOp carries the same extra overhead as in Srcr but reduces the MAC overhead (t_c and t_{ACK} in Section 2). MTOp achieves as much as 13.8 percent higher PDR than Srcr.

Fig. 7b shows the average packet delay versus N . DSR1 experiences the largest packet delay because of its slow packet transmission speed. DSR11 shows the lowest packet delay in the entire range of N . However, it does not represent its true performance because its PDR is low too, particularly at low node density, and the computation of the average packet delay does not take the lost packets into account. MTOp exhibits the lowest packet delay among the rest.

5.3.2 Mixture of Data Rate

To understand how MTOp improves the network performance, we collect statistics about the data rate used when

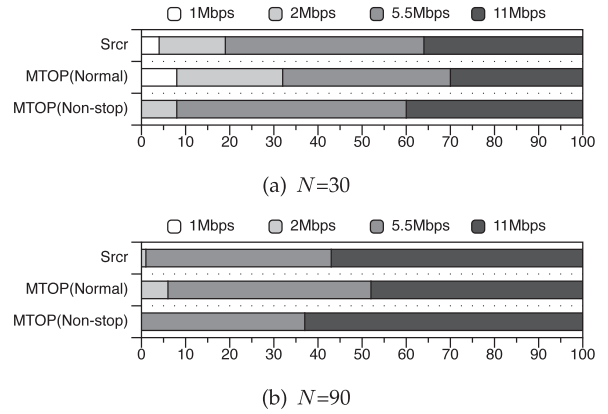


Fig. 8. A mixture of data rate used.

applying the nonstop forwarding. Fig. 8 shows the mixture of data rates for $N = 30$ and $N = 90$. As expected, in Srcr, high rates are used more in high-density network due to the availability of nodes in each node's vicinity.

In comparison, MTOp apparently uses more low-rate transmission as evident in Fig. 8. However, the combination of the two statistics ("Normal" and "Non-stop") results in a similar data. Note that nonstop forwarding in MTOp does not use 1 Mbps. Comparing Figs. 8a and 8b, the mixture of data rate is desirable as more low-rate transmissions are used when network is sparse and vice versa in both Srcr and MTOp.

5.3.3 Frame Drops

Since the fixed rate cases (DSR1 and DSR11) do not possess an adaptive capability and the corresponding performance is not competitive, a more detailed performance measures have been analyzed only for Srcr and MTOp. Figs. 9a, 9b, 9c, and 9d compare the total number of transmissions, total frame drops, frame drop ratio, and duplicate frames, respectively. They have been measured at the MAC layer to include all the forwarding and retransmissions and thus, can be regarded as the actual traffic load in the network. We made the following observations:

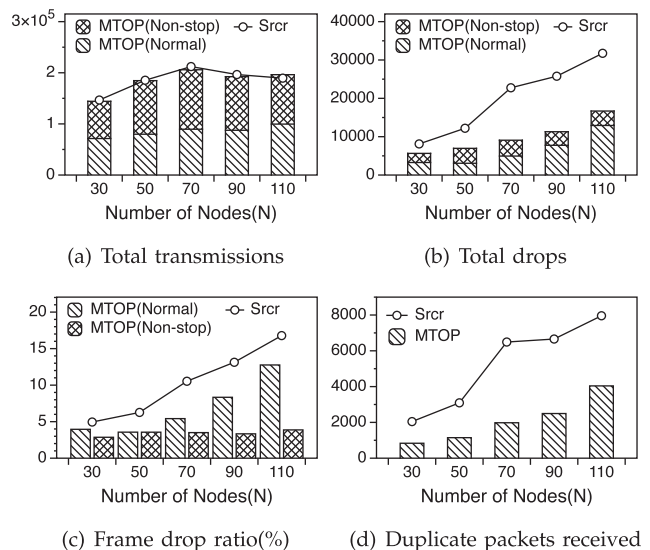


Fig. 9. Frame transmissions and drops in Srcr and MTOp.

TABLE 3
Fairness Index of Srcr and MTOP

	$N=30$	$N=50$	$N=70$	$N=90$	$N=110$
Srcr	0.7353	0.7148	0.7471	0.7398	0.7512
MTOP	0.7320	0.7087	0.7245	0.7203	0.7215

- First, as in Fig. 9a, the total number of transmissions is almost constant for both Srcr and MTOP regardless of N . This is because the traffic intensity is the same. When N is small, low data rates such as 1 and 2 Mbps are used more. This results in less hop count for a given source-destination pair and thus, leads to less number of transmissions.
- Second, in MTOP, more than a half of transmissions are based on nonstop forwarding as shown in Fig. 9a. This observation allows us to estimate the benefit of the implicit ACK (immediate ACK) because all the nonstop forwarding is used as an implicit ACK to the predecessor node. The same number of ACK frames has been saved and the network bandwidth is better utilized for delivering useful data. Assuming that a half of data transmissions are nonstop-forwarded, the benefit of implicit ACK is the reduction of bandwidth usage as much as $\frac{t_{SIFS}+L_{ACK}}{T_1 \text{ or } T_{11}} \times \frac{1}{2}$ or 3.2-13.8 percent.
- Third, while the total number of transmissions is very close between Srcr and MTOP, the latter achieves a higher PDR. This is due to a higher frame drops in Srcr as drawn in Fig. 9b. Compared to MTOP, it drops 43.7-150.5 percent more frames at the MAC layer.
- Fourth, the gap in frame drop can be better explained by investigating the two different frame drops in MTOP. Those with contention (denoted as "Normal" in Fig. 9b) increase rapidly with N , which is similarly observed in Srcr. On the other hand, those without contention (denoted as "Nonstop" in Fig. 9b) are held almost unchanged. Nonstop forwarding is less vulnerable to collisions because it effectively keeps potential interferers silent by taking advantage of the short interframe gap as shown in Fig. 1c.
- Fifth, to see the difference in frame drop more clearly, Fig. 9c shows the frame drop ratio with N . In fact, normal transmissions experience the similar drop ratio in Srcr (4.9-16.8 percent) and MTOP (4.0-12.8 percent), but nonstop forwarding achieves a flat drop ratio (2.9-3.9 percent). This again verifies that MTOP does not cause additional collisions.
- Sixth, the frame drops reported in Fig. 9b are measured at the transmitter. When it does not receive an ACK (either explicit or implicit), it counts it as a drop. As discussed earlier, it is caused by either a lost frame or a lost ACK. The latter can be measured by counting the duplicate frames, which is shown in Fig. 9d. Comparing it with Fig. 9b, it accounts for 25.1-28.6 percent of all frame drops in Srcr. It is 14.8-24.2 percent in MTOP. Less duplicate frames in MTOP explains that implicit ACK in MTOP works reasonably well.

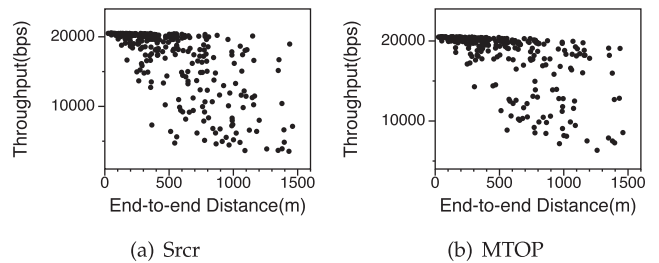


Fig. 10. Distance ($dist_i$) versus throughput (γ_i) (The figure shows a total of 300 flows comprising 30 flows per each of 10 simulation runs when $N = 50$.)

5.3.4 Fairness

Based on the discussion in Section 4.3, we define *space-based fairness index*, F , to measure the balance of total work done on flows in the network, i.e.,

$$F = \frac{(\sum_{i=1}^L (\gamma_i \cdot dist_i))^2}{L \sum_{i=1}^L (\gamma_i \cdot dist_i)^2}, \quad (16)$$

where L is the number of traffic flows. The index value ranges from 0 (completely unfair) to 1 (perfectly fair) [48].

According to our simulation result shown in Table 3, MTOP seems not improve the fairness in comparison to others including Srcr. This is due to the fact that many flows achieve almost 100 percent PDR regardless of the end-to-end distance of the flow when network is lightly loaded. This becomes clearer in Fig. 10, which shows the scatter plot of distance ($dist_i$) and throughput (γ_i). Similar values of F in MTOP and Srcr is contributed by the flows represented by dots on the top in the figure. However, for the rest of the flows, MTOP offers more balanced service to flows depending on their end-to-end distances.

5.3.5 Virtual Carrier Sensing Using RTS/CTS

Virtual carrier sensing helps reduce collisions for nonstop-forwarded packets in MTOP as shown in Fig. 11a. Both MTOP and Srcr drops more packets than in Fig. 9b but Srcr consistently drops more packets than MTOP. However, it is more important to note that nonstop-forwarded packets in MTOP drops rarely and is almost negligible. Nodes become better aware of the multihop forwarding due to the virtual carrier sense and thus, can avoid collisions and reduce packet drops.

One more note is that the number of total drops is much bigger than that in Fig. 9b. This is not surprising because the RTS/CTS exchange itself is an additional overhead and at the same time reduces the spatial resuability of the channel

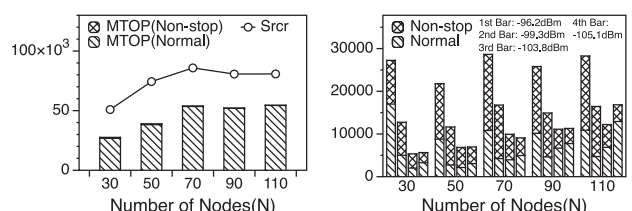


Fig. 11. Total drops (comparing with Fig. 9b).

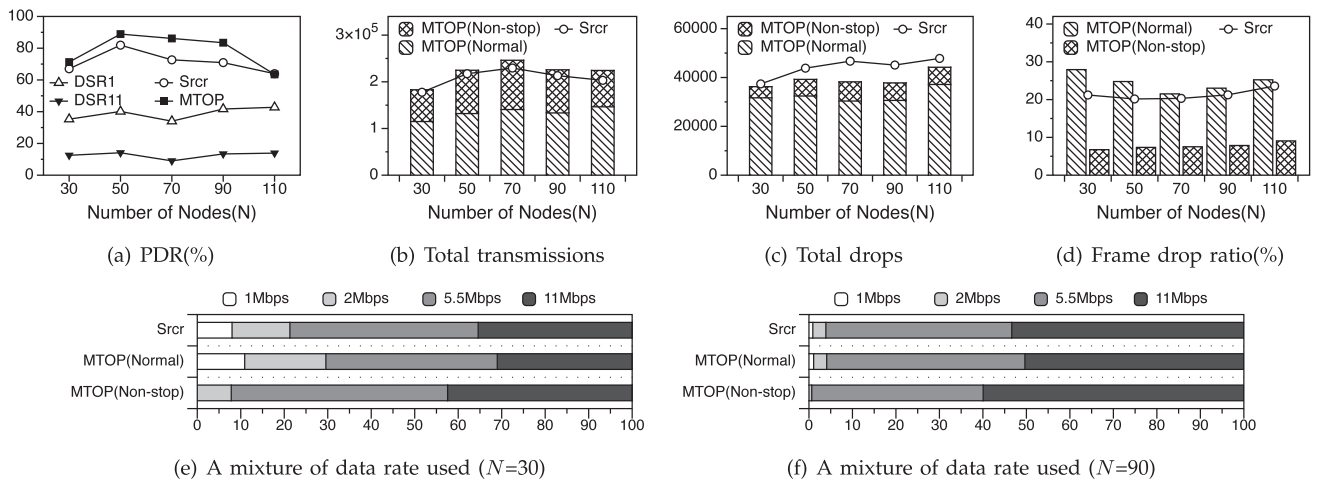


Fig. 12. Performance comparison with Ricean fading ($K = 5$).

due to the more conservative setting of NAV (network allocation vector) for nodes near the receiver.

5.3.6 Effect of Defer Threshold

As discussed in Section 3.3, the defer threshold is an essential parameter in carrier sensing mechanism as it determines neighboring nodes that need to refrain from transmitting. In multirate environment, it is normally set to the value corresponding to the minimum TI distance, which is -105.1 dBm in Table 2. To see the effect of different setting of the defer threshold, we used -103.8 , -99.3 , and -96.2 dBm that correspond to 2, 5.5, and 11 Mbps. As shown in Fig. 11b, a higher threshold generates more collisions. At the defer threshold of -96.2 dBm, the number of packet drops is 1.6-5.4 times more than that of -105.1 dBm. However, the difference is reduced in high density scenario (large N). This is because more communications are made at high rates such as 11 Mbps and the communication at 11 Mbps would not be a problem with the defer threshold corresponding to 11 Mbps.

5.3.7 Effect of Unreliable Links

To see how MTOP performs in a more realistic environment, a set of experiments has been conducted with Ricean model instead of the conventional two-ray ground propagation model used above [49]. According to [50], the Ricean channel is described by the K factor (K), which is defined as the ratio of mean power in dominant component (line-of-sight) over the power in the other scattered paths. We varied K from 0 (harsh channel condition) to 30 (better channel condition) but show the results with $K = 5$ only for brevity. The maximum velocity (v_{max}), which represents the movement speed of surrounding objects, is fixed to 0.5 m/s in our simulation [50].

Fig. 12 shows PDR, total number of transmissions, total frame drops, frame drop ratio, and mixtures of data rate ($N = 30$ and $N = 90$).

- As shown in Fig. 12a, the harsh channel condition impacts all four. PDR reduces by 14.6-21.1 percent and 10.0-31.0 percent in Srcr and MTOP, respectively. MTOP is affected more although the actual PDR is still as much as 13.5 percent higher than Srcr. Note that it impacts DSR11 most severely. DSR11

does not perform well even in high-density scenarios ($N = 110$) because high-rate links (11 Mbps) suffer most in harsh conditions.

- We observed that there are more “Normal” transmissions than “Nonstop” forwarding over Ricean channel in Fig. 12b while this is the opposite in Fig. 9a. While nonstop forwarding in MTOP is supposed to happen over high-rate links, the harsh channel condition makes less use of high-rate links, and so is nonstop forwarding.
- Total number of frame drops increases with Ricean channel, which is particularly prominent at low-density scenario in both Srcr and MTOP as shown in Fig. 12c. In fact, frame drops in Srcr and normal drops in MTOP increase sharply in Fig. 9b but it is almost constant in Fig. 12c. The same can be said based on Figs. 12d and 9c. Frame drops with two-ray model are mainly caused by collisions but those with Ricean channel are caused by channel variations [51]. More frame drops render both Srcr and MTOP to use low-rate links, which is evident in Figs. 12e and 12f.

It can be concluded that the performance gain of MTOP over Srcr is reduced under harsh channel condition because nonstop forwarding over high-rate links gets stopped more often than in better channel condition. This leaves a room for improvement in our future work.

5.3.8 Performance with Various Traffic Conditions

Figs. 13 and 14 show the performance in differently loaded networks by increasing the number of flows (see Fig. 13) and the packet generation rate of each flow (see Fig. 14). More traffic means more transmissions (see Figs. 13b and 14b), more collisions, and more frame drops (see Figs. 13c and 14c). However, MTOP consistently exhibits a better PDR (0.5-16.7 percent in Fig. 13a and 2.0-15.6 percent in Fig. 14a) and less frame drops (31.5-57.5 percent in Fig. 13c and 33.7-56.3 percent in Fig. 14c). In terms of frame drop ratio, “Normal” and “Nonstop” frames are dropped 0.7-4.8 percent and 4.4-12.7 percent less than Srcr, respectively. Therefore, it is concluded that MTOP outperforms Srcr in a wide range of traffic conditions.

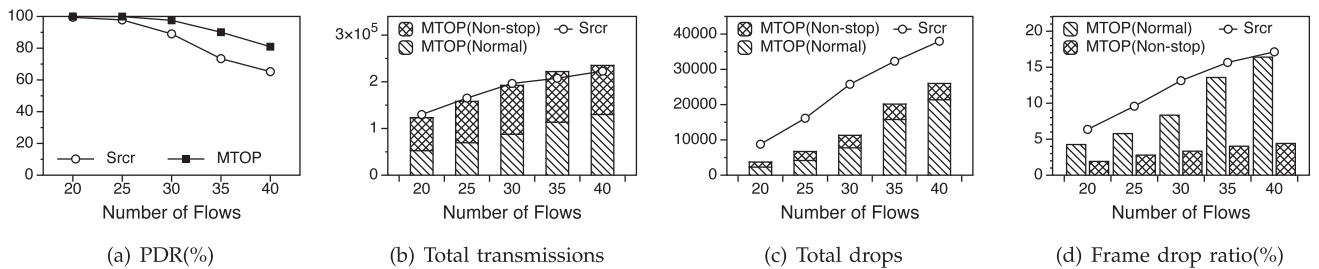


Fig. 13. Impact of traffic load (number of flows).

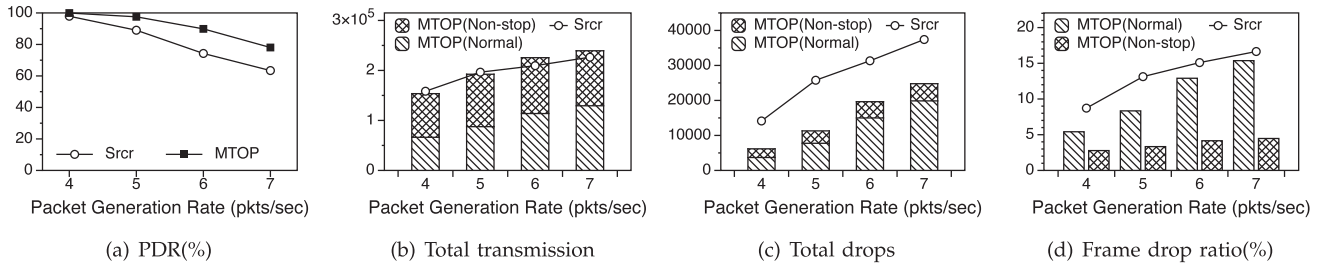


Fig. 14. Impact of traffic load (packet generation rate).

6 CONCLUSION AND FUTURE WORK

Multirate adaptation is a promising tool in wireless multihop networks as the corresponding hardware has been available off-the-shelf. This paper proposes MTOP, which implements nonstop frame forwarding mechanism and achieves low-latency, high-throughput communication. Feasibility of MTOP has been proven via analysis and a small-scale testbed based on USRP/GNU Radio platform. Our performance study based on OPNET network simulator shows that MTOP performs better than fixed-rate scenarios (DSR1 and DSR11) and Ssrc in terms of PDR and packet delay in the entire operating conditions simulated. This is due to the adaptive behavior of MTOP depending on data rate used and the aggressive frame forwarding mechanism along with the reduced MAC overhead.

MTOP opens up several interesting directions of research to pursue. First, the two new concepts, multirate margin and space-based fairness, need a closer investigation as they have a potential to further improve the operation of multihop networks. Second, there are several ways to improve the MTOP. For example, optimal value of h_i and the corresponding network density estimation constitute another future work. Third, MTOP can be usefully employed in multiradio/multichannel networks, typically found in the backhaul of wireless mesh networks. Fourth, it is noted that TXOP and MTOP are not mutually exclusive and can be combined to diversify and maximize the transmission opportunities in multihop networks. When a node transmits a frame, it makes a prudent decision whether to seek an additional transmission opportunity according to TXOP or MTOP.

ACKNOWLEDGMENTS

This research was supported in part by the US National Science Foundation under Grants CNS-1160775 and CNS-1317411. It is also supported by the Basic Science Research Program (2010-0029034) and WCU program (R31-10100), both of which are through the NRF (Korea) funded by the

Ministry of Education, Science, and Technology. This work was presented in part at IEEE INFOCOM 2010 [1].

REFERENCES

- [1] C. Yu, T. Shen, K.G. Shin, J.-Y. Lee, and Y.-J. Suh, "Multihop Transmission Opportunity in Wireless Multihop Networks," *Proc. IEEE INFOCOM*, 2010.
- [2] *Civilian Applications of Unmanned Aircraft Systems (CAUAS)*, 2007, <http://www.cauas.colorado.edu>, 2013.
- [3] T. Zajkowski, S. Dunagan, and J. Eilers, "Small UAS Communications Mission," *Proc. 11th Biennial USDA Forest Service Remote Sensing Applications Conf.*, 2006.
- [4] P. Hui, J. Crowcroft, and E. Yoneki, "BUBBLE Rap: Social-Based Forwarding in Delay Tolerant Networks," *Proc. ACM MobiHoc*, pp. 241-250, May 2008.
- [5] H. Rheingold, *Smart Mobs: The Next Social Revolution*. Perseus Book Group, 2002.
- [6] K. Seada and C. Perkins, "Social Networks: The Killer App for Wireless Ad Hoc Networks?" Technical Report NRC-TR-2006-010, Nokia, Aug. 2006.
- [7] *IEEE Standard 802.11-1999, Part 11: Wireless LAN Medium Access Control (MAC) and Physical Layer (PHY) Specifications*, IEEE, 1999.
- [8] *IEEE Standard 802.11e-2005, Part 11: Wireless Medium Access Control (MAC) and Physical Layer (PHY) Specifications: Medium Access Control (MAC) Enhancements for Quality of Service (QoS)*, IEEE, 2005.
- [9] B. Sadeghi, V. Kanodia, A. Sabharwal, and E. Knightly, "Opportunistic Media Access for Multirate Ad Hoc Networks," *Proc. ACM MobiCom*, pp. 27-35, Sept. 2002.
- [10] G. Tan and J. Guttag, "Time-Based Fairness Improves Performance in Multi-Rate WLAN," *Proc. USENIX Technical Conf.*, 2004.
- [11] I. Tinnirello and S. Choi, "Temporal Fairness Provisioning in Multi-Rate Contention-Based 802.11e WLANs," *Proc. IEEE Sixth Int'l Symp. World of Wireless Mobile and Multimedia Networks (WoWMoM)*, pp. 220-230, June 2005.
- [12] J. Bicket, D. Aguayo, S. Biswas, and R. Morris, "Architecture and Evaluation of an Unplanned 802.11b Mesh Network," *Proc. ACM MobiCom* pp. 31-42, Aug./Sept. 2005.
- [13] OPNET Modeler, <http://www.opnet.com>, 2013.
- [14] Universal Software Radio Platform, <http://www.ettus.com>, 2013.
- [15] GNU Radio Project, <http://www.gnuradio.org/trac>, 2013.
- [16] A. Kamerman and L. Monteban, "WaveLAN-II: A High-Performance Wireless LAN for the Unlicensed Band," *Bell Labs Technical J.*, vol. 2, no. 3, pp. 118-133, 1997.
- [17] M. Lacage, M.H. Manshaei, and T. Turletti, "IEEE 802.11 Rate Adaptation: A Practical Approach," *Proc. ACM Seventh ACM Int'l Symp. Modeling, Analysis and Simulation of Wireless and Mobile Systems (MSWiM)*, 2004.

- [18] A. Akella, G. Judd, S. Seshan, and P. Steenkiste, "Self-Management in Chaotic Wireless Deployments," *Proc. ACM MobiCom*, pp. 185-199, Aug./Sept. 2005.
- [19] G. Holland, N. Vaidya, and P. Bahl, "A Rate-Adaptive MAC Protocol for Multi-Hop Wireless Networks," *Proc. ACM MobiCom*, pp. 236-251, July 2001.
- [20] Z. Ji, Y. Yang, J. Zhou, M. Takai, and R. Bagrodia, "Exploiting Medium Access Diversity in Rate Adaptive Wireless LANs," *Proc. ACM MobiCom*, 2004.
- [21] S.T. Sheu, Y. Tsai, and J. Chen, "MR2RP: The Multi-Rate and Multi-Range Routing Protocol for IEEE 802.11 Ad Hoc Wireless Networks," *Wireless Networks*, vol. 9, no. 2, pp. 165-177, 2003.
- [22] H. Zhai and Y. Fang, "Physical Carrier Sensing and Spatial Reuse in Multirate and Multihop Wireless Ad Hoc Networks," *Proc. IEEE INFOCOM*, pp. 1-12, Apr. 2006.
- [23] B. Awerbuch, D. Holmer, and H. Rubens, "The Medium Time Metric: High Throughput Route Selection in Multi-Rate Ad Hoc Wireless Networks," *Mobile Networks and Applications*, vol. 11, pp. 253-266, 2006.
- [24] R. Draves, J. Padhye, and B. Zill, "Routing in Multi-Radio, Multi-Hop Wireless Mesh Networks," *Proc. ACM MobiCom*, pp.114-128. Sept./Oct. 2004.
- [25] Strix Systems, http://www.strixsystems.com/products/datasheets/StrixWhitepaper_Multihop.pdf, Mar. 2008.
- [26] C.E. Perkins and P. Bhagwat, "Highly Dynamic Destination-Sequenced Distance-Vector Routing (DSDV) for Mobile Computers," *ACM SIGCOMM Computer Comm. Rev.*, vol. 24, no. 4, pp. 234-244, 1994.
- [27] D. Johnson and D. Maltz, "Dynamic Source Routing in Ad-Hoc Wireless Networks," *Mobile Computing*, T. Imielinski and H. Korth, eds., Kluwer Academic, 1996.
- [28] S. Biswas and R. Morris, "Opportunistic Routing in Multi-Hop Wireless Networks," *Proc. Second Workshop Hot Topics in Networks (HotNets-II)*, 2003.
- [29] M. Zorzi and R. Rao, "Geographic Random Forwarding (GeRaF) for Ad Hoc and Sensor Networks: Energy and Latency Performance," *IEEE Trans. Mobile Computing*, vol. 2, no. 4, pp. 349-365, Oct.-Dec. 2003.
- [30] K. Jamieson, H. Balakrishnan, and Y.C. Tay, "Sift: A MAC Protocol for Event-Driven Wireless Sensor Networks," *Proc. Third European Workshop Wireless Sensor Networks (EWSN)*, 2006.
- [31] T. Li, Q. Ni, D. Malone, D. Leith, Y. Xiao, and T. Turletti, "Aggregation with Fragment Retransmission for Very High-Speed WLANs," *IEEE/ACM Trans. Networks*, vol. 17, no. 2, pp. 591-604, Apr. 2009.
- [32] M. Heusse, F. Rousseau, G. Berger-Sabbatel, and A. Duda, "Performance Anomaly of 802.11b," *Proc. IEEE INFOCOM*, vol. 2, pp. 836-843, Mar./Apr. 2003.
- [33] "Orinoco 11b Client PC Card Spec.," <http://www.proxim.com/learn/library/datasheets/11bpccard.pdf>, 2003.
- [34] K. Marquess, "Physical Model Sub-Group Discussion and Questions," Technical Report IEEE 802.15/138R0, 1999.
- [35] *IEEE Standard 802.15.2-2003, Part 15.2: Coexistence of Wireless Personal Area Networks with Other Wireless Devices Operating in Unlicensed Frequency Bands*, IEEE, 2003.
- [36] C. Yu, K.G. Shin, and L. Song, "Link-Layer Salvaging for Making Routing Progress in Mobile Ad Hoc Networks," *Proc. ACM MobiHoc*, pp. 242-254, May 2005.
- [37] M. Bertocco, G. Gamba, and A. Sona, "Experimental Optimization of CCA Thresholds in Wireless Sensor Networks in the Presence of Interference," *Proc. IEEE Electromagnetic Compatibility (EMC) Europe*, 2007.
- [38] R. Gummadi, D. Wetherall, B. Greenstein, and S. Seshan, "Understanding and Mitigating the Impact of RF Interference on 802.11 Networks," *Proc. ACM Special Interest Group on Data Comm. (SIGCOMM '07)*, pp. 385-396, Aug. 2007.
- [39] S. Narayanaswamy, V. Kawadia, R.S. Sreenivas, and P.R. Kumar, "Power Control in Ad-Hoc Networks: Theory, Architecture, Algorithm and Implementation of the COMPOW Protocol," *Proc. European Wireless Conf.*, Feb. 2002.
- [40] A. Jow, C. Schurgers, and D. Palmer, "CalRadio: A Portable, Flexible 802.11 Wireless Research Platform," *Proc. ACM First Int'l Workshop System Evaluation for Mobile Platforms (MobiEval)*, pp. 49-54, June 2007.
- [41] K.A. Jamieson, "The SoftPHY Abstraction: From Packets to Symbols in Wireless Network Design," PhD dissertation, Massachusetts Inst. Tech., June 2008.
- [42] GNU Radio Source, http://gnuradio.org/trac/browser/gnuradio/trunk/usrp/fpga/sdr_lib/adc_interface.v, 2013.
- [43] J. Lee, W. Kim, S.J. Lee, D. Jo, J. Ryu, T. Kwon, and Y. Choi, "An Experimental Study on the Capture Effect in 802.11a Networks," *Proc. Second ACM Int'l Workshop Wireless Network Testbeds, Experimental Evaluation and Characterization (WinTECH)*, pp. 19-26, Sept. 2007.
- [44] BBN ADROIT Project, <http://acert.ir.bbn.com/projects/adroit>, 2013.
- [45] R. Dhar, G. George, A. Malani, and P. Steenkiste, "Supporting Integrated MAC and PHY Software Development for the USRP SDR," *Proc. IEEE Workshop Networking Technologies for Software Defined Radio (SDR) Networks*, 2006.
- [46] T. Schmid, O. Sekkat, and M.B. Srivastava, "An Experimental Study of Network Performance Impact of Increased Latency in Software Defined Radios," *Proc. ACM Second Int'l Workshop Wireless Network Testbeds, Experimental Evaluation and Characterization (WinTECH)*, 2007.
- [47] J. Broch, D.A. Maltz, D.B. Johnson, Y.-C. Hu, and J. Jetcheva, "A Performance Comparison of Multi-Hop Wireless Ad Hoc Network Routing Protocols," *Proc. ACM MobiCom*, 1998.
- [48] R. Jain, D. Chiu, and W. Hawe, "A Quantitative Measure of Fairness and Discrimination for Resource Allocation in Shared Systems," Technical Report TR-301, Digital Equipment Corp., Aug. 1984.
- [49] R.J. Punnoose, P.V. Nikitin, and D.D. Stancil, "Efficient Simulation of Ricean Fading within a Packet Simulator," *Proc. IEEE 52nd Vehicular Technology Conf. (VTC-Fall)*, 2000.
- [50] Z. Chen, X. Yang, and N.H. Vaidya, "Dynamic Spatial Backoff in Fading Environments," *Proc. IEEE Fifth Int'l Conf. Mobile Ad Hoc and Sensor Systems (MASS)*, 2008.
- [51] J. Kim, S. Kim, S. Choi, and D. Qiao, "CARA: Collision-Aware Rate Adaptation for IEEE 802.11 WLANs," *Proc. IEEE INFOCOM*, Apr. 2006.



Jeong-Yoon Lee received the BS degree in computer science and engineering from Dongguk University, Seoul, Korea, in 2006. He is currently working toward the PhD degree in the Department of Computer Science and Engineering at Pohang University of Science and Technology, Korea. His research interests include MAC and routing protocols, cooperative communication, and network coding in wireless multihop networks. He is a student member of the IEEE.



Chansu Yu received the BS and MS degrees in electrical engineering from Seoul National University, Korea, in 1982 and 1984, respectively, and the PhD degree in computer engineering from Pennsylvania State University in 1994. He is currently a professor in the Department of Electrical and Computer Engineering at Cleveland State University (CSU), Ohio. Before joining CSU, he was on the research staff at LG Electronics. He has been on the program committee or organizing committee of many conferences and workshops, including cochair of the IEEE Percom Workshop on Pervasive Wireless Networking during the last eight years and cochair of the 2013 Fourth International Conference on Network of the Future. He has authored/coauthored more than 110 technical papers and book chapters in the areas of mobile networks, performance evaluation, and parallel and distributed computing. He is a senior member of the IEEE.



Kang G. Shin is the Kevin & Nancy O'Connor professor of computer science in the Department of Electrical Engineering and Computer Science, The University of Michigan, Ann Arbor. His current research interests include computing systems and networks as well as embedded real-time and cyber-physical systems, all with emphasis on timeliness, security, and dependability. He has supervised the completion of 73 PhDs, and authored/coauthored more than

800 technical articles (about 300 of these in archival journals), and one textbook. He has received more than 20 patents or invention disclosures and numerous awards, including Best Paper Awards from the 2011 ACM International Conference on Mobile Computing and Networking (MobiCom '11), the 2011 IEEE International Conference on Autonomic Computing, the 2010 and 2000 USENIX Annual Technical Conferences, the 2003 IEEE Communications Society William R. Bennett Prize Paper Award, and the 1987 Outstanding IEEE Transactions of Automatic Control Paper Award. He has also received several institutional awards, including the Research Excellence Award in 1989, the Outstanding Achievement Award in 1999, the Distinguished Faculty Achievement Award in 2001, the Stephen Attwood Award in 2004 from The University of Michigan (the highest honor bestowed to Michigan Engineering faculty), a Distinguished Alumni Award of the College of Engineering, Seoul National University in 2002, the 2003 IEEE RTC Technical Achievement Award, and the 2006 Ho-Am Prize in Engineering (the highest honor bestowed to Korean-origin engineers). He is a fellow of the IEEE.



Young-Joo Suh received the BS and MS degrees in electronics engineering from Hanyang University, Seoul, Korea, in 1985 and 1987, respectively, and the PhD degree in electrical and computer engineering from the Georgia Institute of Technology, Atlanta, in 1996. He is currently a professor in the Department of Computer Science and Engineering at the Pohang University of Science and Technology, Korea. From 1988 to 1990, he was a

research engineer at the Central Research Center of LG Electronics, Inc., Seoul, Korea. From 1990 to 1993, he was an assistant professor in the Department of Computer Science and Engineering at the Chung-Cheong College, Korea. After receiving the PhD degree, he worked as a postdoctoral researcher in the Computer Systems Research Laboratory in the School of Electrical and Computer Engineering at the Georgia Institute of Technology from 1996 to 1997. From 1997 to 1998, he was a research fellow of the Real-Time Computing Laboratory in the Department of Electrical Engineering and Computer Science at the University of Michigan. His current research interests include wireless LAN MAC protocols, mobility management, ad hoc networks, and 4G wireless mobile networks. He is a member of the IEEE and the IEEE Communications Society.

▷ **For more information on this or any other computing topic, please visit our Digital Library at www.computer.org/publications/dlib.**